

ORIGINAL ARTICLES

The Probability Of Karun River Environmental Pollution Due To Seismic Response Of Masjed Soleyman Dam

Zaniar Tokmechi

Department of Civil Engineering, Mahabad Branch, Islamic Azad University, Mahabad, Iran

ABSTRACT

The Masjed Soleyman Dam previously named "Godar-e Landar" is a dam in Iran on the Karun river. It is about 164 meters (538 ft) high and generates 2,000 MW of power, and its reservoir holds 228,000,000 cubic meters of water. The Karun river is Iran's most effluent, and the only navigable, river. It is 720 km long. It rises in the Zard Kuh mountains of the Bakhtiari district in the Zagros Range, receiving many tributaries, such as the Dez and the Kuhrang, before passing through the capital of the Khuzestan Province of Iran, the city of Ahwaz. In this paper, the probability of environmental pollution due to heavy metals caused by Masjed soleyman dam failure is studied. Finite Element and ZENGAR methods are used to analyze the probability of pollution at dam downstream. Different dam cross sections and various loading conditions are considered to study the effects of these factors on the seismic behavior of the dam. Results show that the effect of the highest cross section is not the most significant for heavy metals pollution at the dam down stream. Pollution coefficient due to stress along Y axis (S_y) is always the determinant pollution. While, in all sections S_x and S_y are the determinant parameter affecting downstream heavy metal pollution and normally are bigger than S_z . And, S_z which can never be a determinant. According to results, when the earthquake accelerations are bigger, maximum pollution coefficient due to tensile stress at dam basement is increased. While, the pollution due the maximum compressive stress at dam basement depends on both earthquake acceleration and loading condition.

Key words: Environmental pollution, Seismic Response, Masjed soleyman dam, ZENGAR, FEM.

Introduction

The Masjed soleyman dam is a rockfill structure with a clay core built for the Iran Water and Power Resources Development Co. The dam was named after the town of Masjed-Soleyman, about 25 kilometres (16 mi) away. The spillway gates are believed to be the largest of their kind in the world.

The Karun river continues toward the Persian Gulf, forking into two primary branches on its delta: the Bahmanshir and the Haffar that joins the Shatt al-Arab (Arvand Rud in Persian), emptying into the Persian Gulf. The important Island of Abadan is located between these two branches of the Karun. The port city of Khorramshahr is divided from the Island of Abadan by the Haffar branch.

The seismic action on dams is the most important to be considered in dams safety studies and its effects on the environmental pollution (United States Army Corps of Engineers, 1990). In 21st century, hydraulic power exploitation and hydraulic engineering construction have been improved in many countries. Some high dams over 200m, even 300m in height, have been built in many areas of the world (Jianping *et al.*, 2006).

Pollution is the introduction of contaminants into a natural environment that causes instability, disorder, harm or discomfort to the ecosystem i.e. physical systems or living organisms (Mohsenifar *et al.*, 2011; Allahyaripur *et al.*, 2011). Pollution can take the form of chemical substances or energy, such as noise, heat, or light. Pollutants, the elements of pollution, can be foreign substances or energies (Arabian and Entezarei, 2011), or naturally occurring; when naturally occurring, they are considered contaminants when they exceed natural levels (Arbabian *et al.*, 2011; Hosseini and Sabouri, 2011). Pollution is often classed as point source or no point source pollution.

Pollution has always been with us. According to articles in different journals soot found on ceilings of prehistoric caves provides ample evidence of the high levels of pollution that was associated with inadequate ventilation of open fires. The forging of metals appears to be a key turning point in the creation of significant air pollution levels outside the home (Core samples of glaciers in Greenland indicate increases in pollution associated with Greek, Roman and Chinese metal production.

According to the statistics, the construction regions in many areas, are notable for their high environmental pollution (Wang and Li, 2006; Qasim *et al.*, 2010 a; Qasim *et al.*, 2010 b). Therefore, environmental studies affected by the seismic safety of large dams is one of the key problems that need to be solved in the design of

dams. While, difficulties exist in determining the seismic response of dams (United States Army Corps of Engineers, 1995). The most important difficulty is dams complex geometry and forms, motivated by the topography and geotechnical character of the implantation zone and controlling the project pollution effects.

According to the previous studies, usually 2D models corresponding to the higher section the dam have been used in the structural seismic analyses of the dams (Fenves and Chopra, 1984). While, normally there is a lot of variation in the dam foundation geometry which can be extremely make the study of the dam downstream pollution difficult.

In this paper, the probability of environmental pollution caused by Masjed soleyman dam failure is studied. Finite Element and ZENGAR methods are used to analyze the probability of pollution at dam downstream. Different dam cross sections and various loading conditions are considered to study the effects of these factors on the probability of environmental pollution due to seismic behavior of the dam.

Materials And Methods

Masjed Soleyman Dam:

The Masjed Soleyman Dam previously named "Godar-e Landar" is a dam in Iran on the Karun river. It is about 164 meters (538 ft) high and generates 2,000 MW of power, and its reservoir holds 228,000,000 cubic meters of water. Figure 1 shows Masjed Soleyman dam.



Fig. 1: Masjed soleyman dam

Karun River:

The Karun is Iran's most effluent, and the only navigable, river. It is 720 km long. It rises in the Zard Kuh mountains of the Bakhtiari district in the Zagros Range, receiving many tributaries, such as the Dez and the Kuhrang, before passing through the capital of the Khuzestan Province of Iran, the city of Ahwaz. Figure 2 shows the Karun river map.



Fig. 2: Karun river map

The Karun continues toward the Persian Gulf, forking into two primary branches on its delta: the Bahmanshir and the Haffar that joins the Shatt al-Arab (Arvand Rud in Persian), emptying into the Persian Gulf. The important Island of Abadan is located between these two branches of the Karun. The port city of Khorramshahr is divided from the Island of Abadan by the Haffar branch.

In the Biblical tradition, Karun is to be identified with Pishon, one of the four rivers of Eden/Paradise. The others being Tigris, Euphrates and the Karkheh ("Gihon" of the Biblical story). In the early classical times, Karun was known as the Pasitigris, which may be pointing etymologically to the source of the Biblical name, Pishon. The modern medieval and modern name, Karun, is a corruption of the name, Kuhrang which is still maintained by one of the two primary tributaries of the Karun.

Karun River Course:

It originates in the Zagros Mountains of western Iran, on the slopes of 14,921-foot (4,548 m) Zard-Kuh. The river flows south and west through several prominent mountain ridges, and receives additional water from the Vanak on the south bank and the Bazuft on the north. These tributaries add to the catchments of the river above the Karun-4 Dam. Downstream 25 kilometers (16 mi), the Karun widens into the reservoir formed by the Karun-3 Dam. The Khersan flows into an arm of the reservoir from the southeast. The river passes through this reservoir and flows through a narrow canyon, now in a northwest direction, past Izeh, eventually winding into the Sussan Plain. The Karun then turns north into the reservoir of Masjed soleyman Dam (Karun-1), which floods the river's defile to the southwest. The Karun flows southwest into the impoundment of Masjed Soleyman Dam, then turns northwest. Finally, it leaves the foothills and flows south past Shushtar and its confluence with the Dez. It then bends southwest and bisects the city of Ahvaz, and south through farmland to its mouth on the Shatt Al-Arab river at Khorramshahr, where its water, together with that of the Tigris and Euphrates, turns sharply southwest to flow to the Persian Gulf.

Karun River Basin:

The largest river by discharge in Iran, the Karun River's watershed covers 65,230 square kilometers in parts of two Iranian provinces. The river is around 950 kilometers long and has an average discharge of 575 cubic meters per second. The largest city on the river is Ahvaz, with over 1.3 million inhabitants. Other important cities include Shushtar, Khorramshahr (a port), Masjed-Soleyman, and Izeh.

Much of Khuzestan's transport and resources are connected in one way or another to the Karun. Since the British first discovered oil at Masjed-Soleyman, the Karun has been an important route for the transport of petroleum to the Persian Gulf, and remains an important commercial waterway. Water from the Karun provides irrigation to over 280,000 hectares of the surrounding plain and a further 100,000 hectares are planned to receive water. Figure 3 shows the river passing Khoramshahr city.



Fig. 3: Karun river passing Ahvaz

Karun River History:

The Karun River valley was once inhabited by the Elamite civilization which rose about 2,700 B.C. In several points in history, Mesopotamian civilizations such as Ur and Babylon overthrew the Elamites and gained control of the Karun and its surroundings in modern Khuzestan. However, the Elam empire lasted until about 640 B.C., when the Assyrians overran it. The city of Susa, near the modern city of Shush between the Dez and

Karkheh rivers, was one of their largest before it was destroyed by the invaders. Figure 4 shows Derelict vessels

and a bridge over the Karun in Khorramshahr.



Fig. 4: Derelict vessels and a bridge over the Karun in Khorramsha

The first known major bridge across the river was built by the Roman captives that included its emperor Valerian, whence the name of the bridge and dam Band-e Kaisar, "Caesar's dam"--at Shushtar (3rd century AD).

In two of several competing theories about the origins and location of the Garden of Eden the Karun is presumed to be the Gihon River that is described in the Biblical book of Genesis. The strongest of these theories propounded by archaeologist Juris Zarins places the Garden of Eden at the northern tip of the Persian Gulf, fed by the four rivers Tigris, Euphrates, Gihon Karun and Pishon (Wadi Al-Batin).

The name of the river is derived from the mountain peak, Kuhrang, that serves as its source.

Earthquake and ZENGAR Method:

Earthquake as a special and challengeable load condition is one of the most significant loads that is considered in the dam designing and its effects could not be negligible. In this paper, ZENGAR method is used to model the earthquake loading condition (Omran and Tokmechi, 2008). According to this method, hydrodynamic pressure of water can be derived by the equation 1.

$$P = C.\alpha_{h} \cdot \gamma_{W} H \tag{1}$$

where α_h is the maximum horizontal acceleration of the earthquake, γ_w is water mass density , H is the water depth and C is a coefficient which is given by

$$C = \frac{C_m}{2} \left(\frac{Z}{H} (2 - \frac{Z}{H}) - \sqrt{\frac{Z}{H} (2 - \frac{Z}{H})} \right)$$
 (2)

where Z is the depth of the point from the water surface and C_m is a coefficient which is given by

$$C_m = 0.73(\frac{90 - \phi}{90})\tag{3}$$

where \square is the upstream slope.

The inertia load due to the vertical acceleration of the earthquake can be also given by

$$E = \alpha_{\mathcal{V}}.W \tag{4}$$

where α_v is the maximum vertical acceleration of the earthquake and W is the weight of the dam.

In this study, a sample earthquake condition properties have been taken as shown in Table 1 (Omran and Tokmechi, 2008). Also, eight different loading conditions, mentioned in Table 2, have been considered to study the seismic response of the dam (Omran and Tokmechi, 2008).

Table 1. Earthquake Condition

Earthquake Level	Maximum Horizontal Acc. (g)	Maximum Vertical Acc. (g)
DBL	0.28	0.20
MDL	0.34	0.25
MCL	0.67	0.55

Table	2.	Loading	Conditions
-------	----	---------	------------

Loading Condition	Body Weight	Hydrostatic Pressure	Uplift Pressure	Earthquake
LC1	*	-	*	-
LC2	*	*	*	-
LC3	*	*	*	DBL (1 st mode ^I)
LC4	*	*	*	DBL (2 nd mode II)
LC5	*	*	*	MDL (1 st mode)
LC6	*	*	*	MDL (2 nd mode)
LC7	*	*	*	MCL (1 st mode)
LC8	*	*	*	MCL (2 nd mode)

- Earthquake inertia loading and dam body weight act in the same direction I:
- Earthquake inertia loading and dam body weight act in the apposite direction

Finite Element Method:

In this study, Constant Strain Triangle element is used (Chandrupatla, 1997). Equation 5 is used to calculate the element stresses. The calculated stress is used as the value at the center of each element.

$$\sigma = DBq \tag{5}$$

Where D is material property matrix, B is element strain displacement matrix, and q is element nodal displacement from the global displacements vector Q.

For plane strain conditions, the material property matrix is given by Equation 6.

$$D = \frac{E}{(1+\nu)(1-2\nu)} \begin{bmatrix} 1-\nu & \nu & 0\\ \nu & 1-\nu & 0\\ 0 & 0 & 1-2\nu/2 \end{bmatrix}$$
 (6)

Element strain-displacement matrix is given by Equation 7.

Element strain-displacement matrix is given by Equation 7.
$$B = \frac{1}{\det J} \begin{bmatrix} y_{23} & 0 & y_{31} & 0 & y_{12} & 0 \\ 0 & x_{32} & 0 & x_{13} & 0 & x_{21} \\ x_{32} & y_{23} & x_{13} & y_{31} & x_{21} & y_{12} \end{bmatrix}$$
(7)

In which, J is Jacobian matrix, and the points 5, 6, and 7 are ordered in a counterclockwise manner. Jacobian matrix is given by Equation 8.

$$J = \begin{bmatrix} x_{13} & y_{13} \\ x_{23} & y_{23} \end{bmatrix}$$
 (8)

Global displacements vector Q is given by Equation 9.

$$KQ = F$$
 (9)

In which, K and F are modified stiffness matrix and force vector, respectively. The global stiffness matrix K is formed using element stiffness matrix ke which is given by Equation 10.

$$k^e = t_e A_e B^T D B \tag{10}$$

In which, te and Ae are element thickness and element area, respectively.

Results And Discusion

Seismic Response:

Using Finite Element, ZENGAR and probability studies methods, study of the probability of environmental pollution due to Masjed soleyman dam failure has been done and different loading conditions were considered. Fig. 5 to Fig. 15 show the probability of environmental pollution due to failure (Named PEP) caused by maximum compressive stress values in different cross sections. The PEP due to maximum tensile stress values are also shown in Fig. 16 to Fig. 26. The PEP due to vertical stress distribution across dam basement due to different loading conditions are the other key factors for controlling dam safety, and they are shown in Fig. 27 to Fig. 37. In all Figures S_x, S_y and S_z are stand for PEP due to stress along X, Y, and Z axis,

As it can be seen from Fig. 5 to Fig. 15, the PEP due to maximum compressive stress changes due to different loading conditions are similar for different cross sections. While, comparing Fig. 20, Fig. 22 and Fig.

25 there is no response similarity for different cross sections and the PEP due to maximum tensile stress changes are vary from a cross section to another.

It is clear from Fig. 5 to Fig. 26 that the first modes of the earthquake, LC3, LC5 and LC7, develop PEP due to bigger compressive stress. While, the second modes of the earthquake, LC4, LC6 and LC8, develop bigger PEP due to tensile stress. That means for the safety study of RCC dams both modes of earthquake should be analyzed. In addition, Fig. 5 to Fig. 26 show that when the earthquake accelerations are bigger, both PEP due to maximum tensile and compressive stress of dam body are increased.

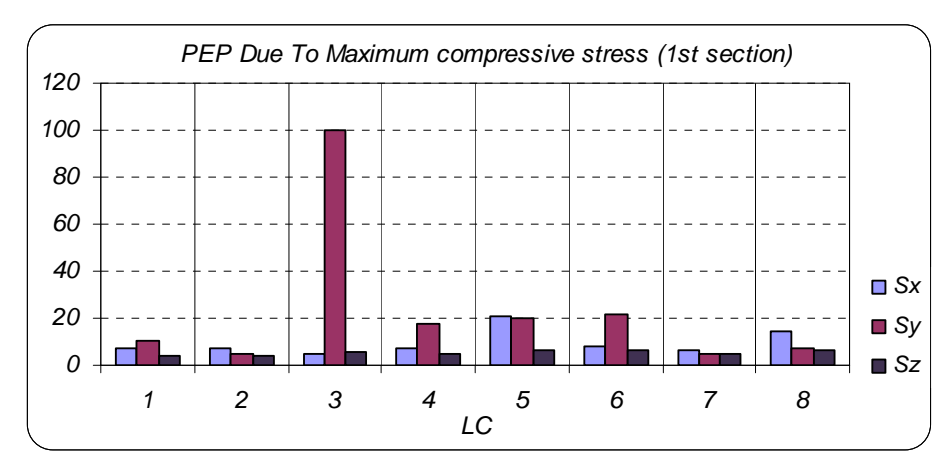


Fig. 5: PEP Due To Maximum compressive stress (1st section)

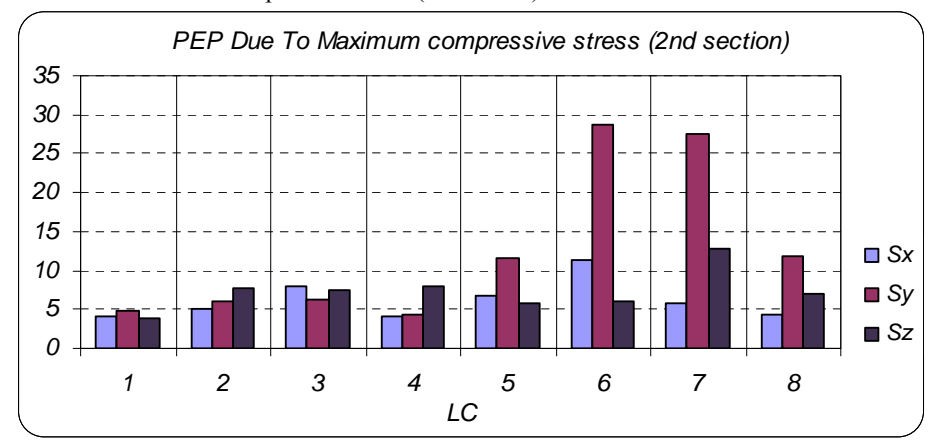


Fig. 6: PEP Due To Maximum compressive stress (2nd section)

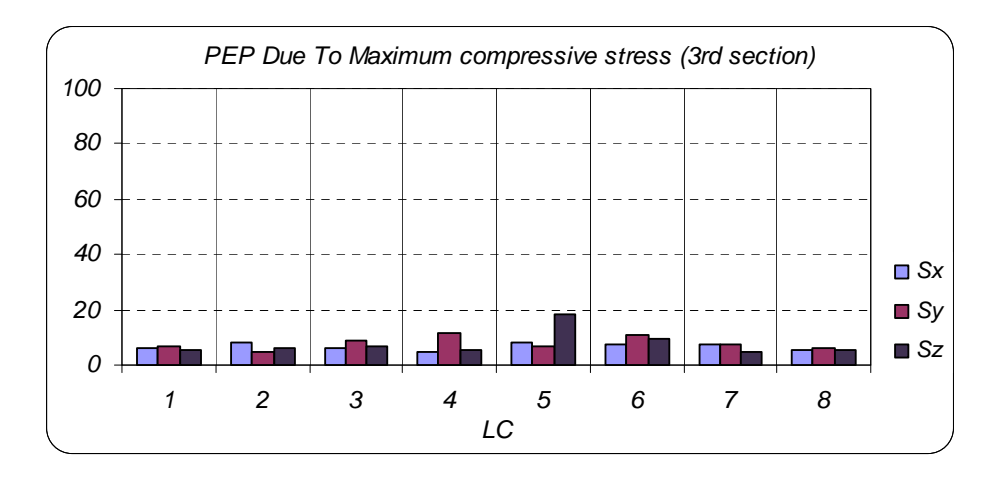


Fig. 7: PEP Due To Maximum compressive stress (3rd section)

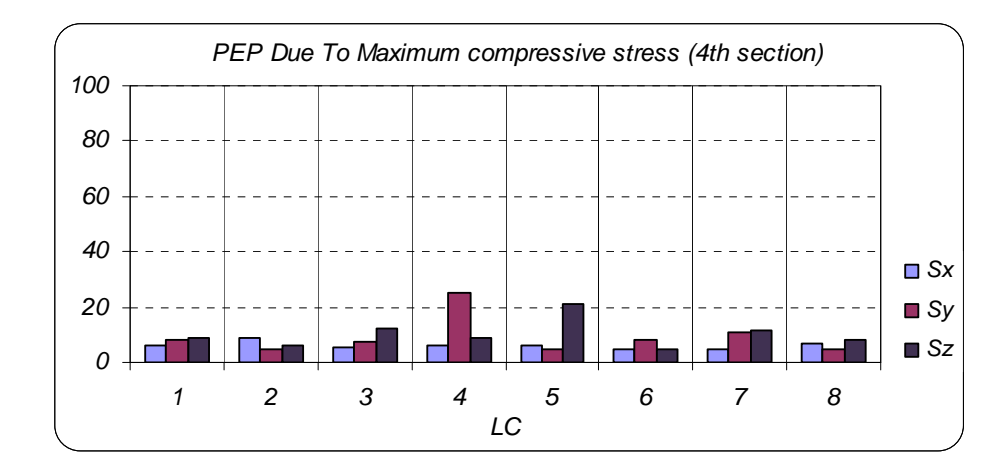


Fig. 8: PEP Due To Maximum compressive stress (4th section)

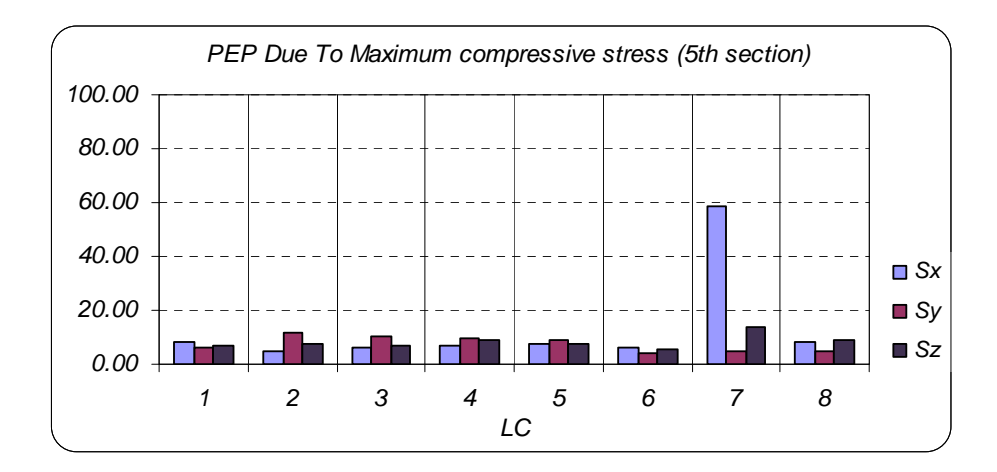


Fig. 9: PEP Due To Maximum compressive stress (5th section)

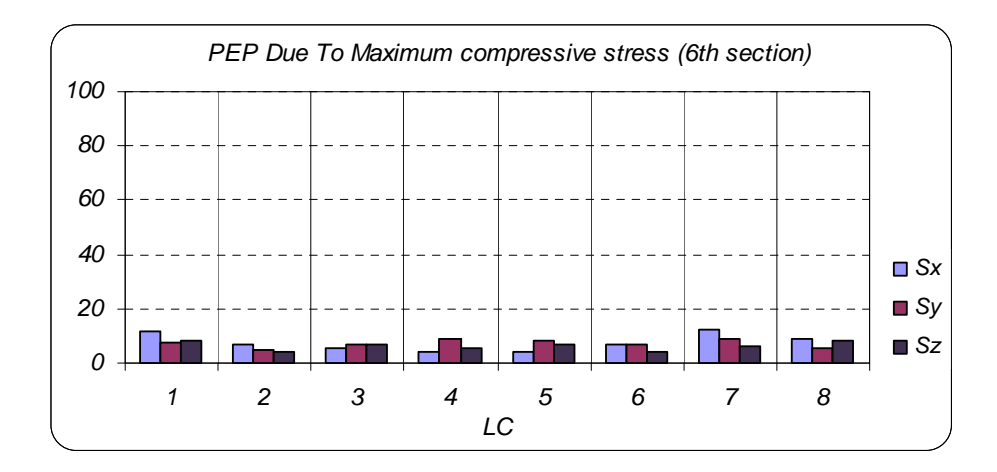


Fig. 10: PEP Due To Maximum compressive stress (6th section)

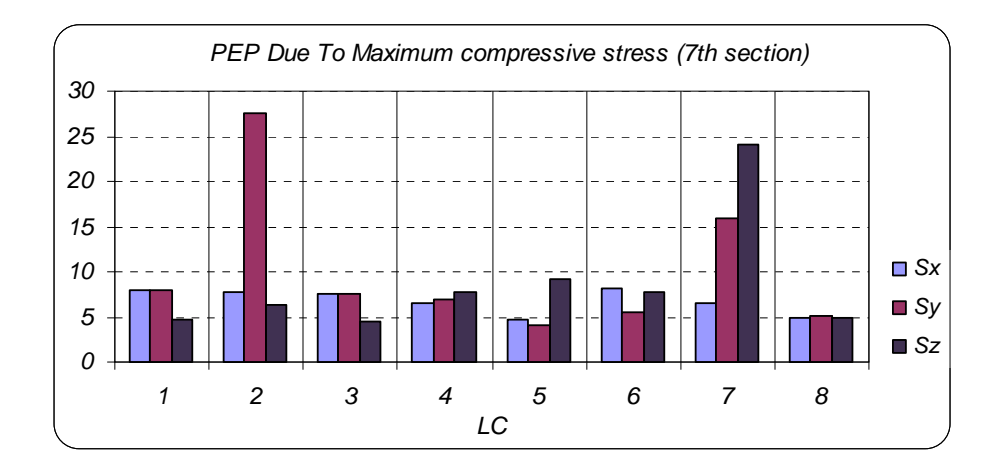


Fig. 11: PEP Due To Maximum compressive stress (7th section)

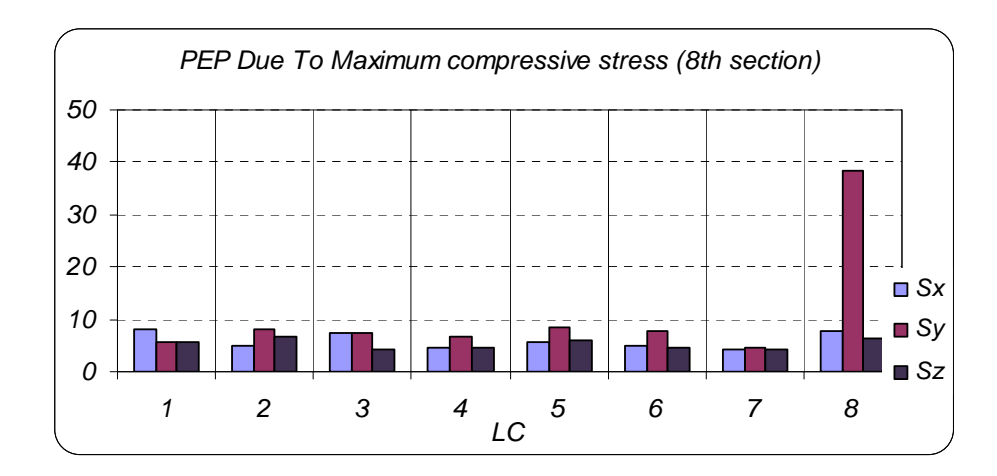


Fig. 12: PEP Due To Maximum compressive stress (8th section)

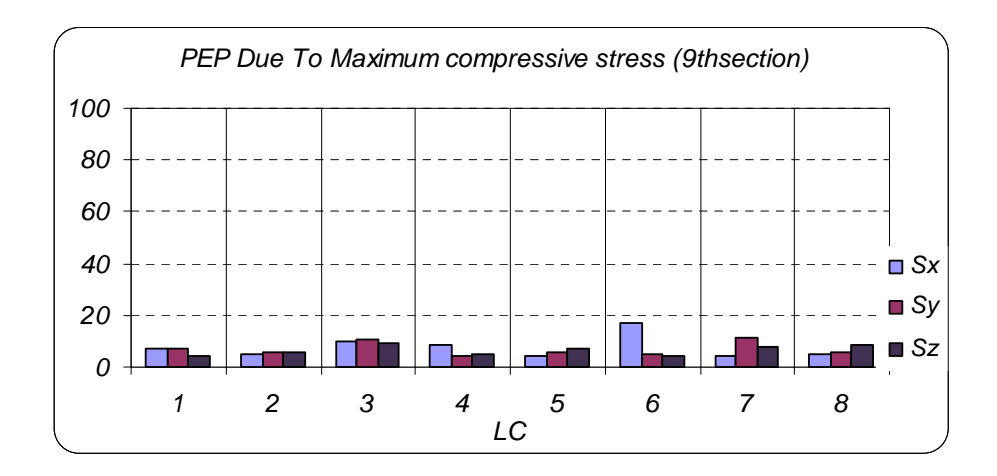


Fig. 13: PEP Due To Maximum compressive stress (9th section)

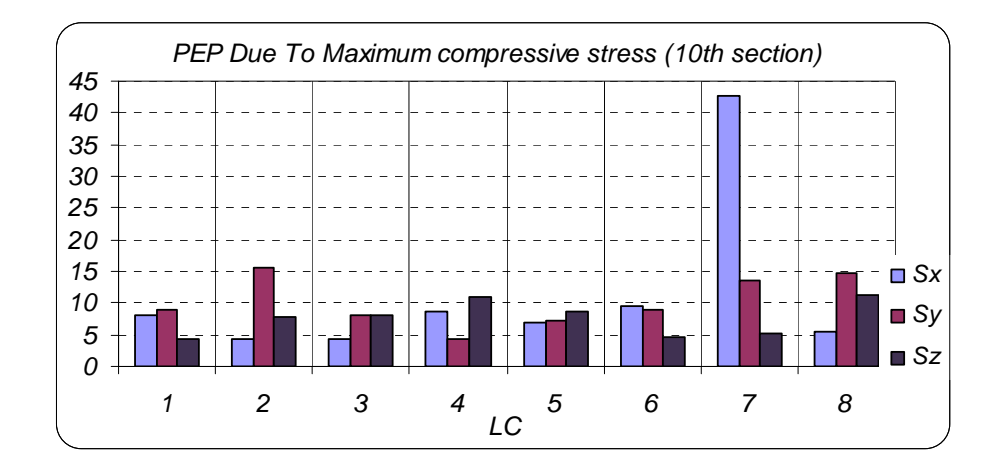


Fig. 14: PEP Due To Maximum compressive stress (10th section)

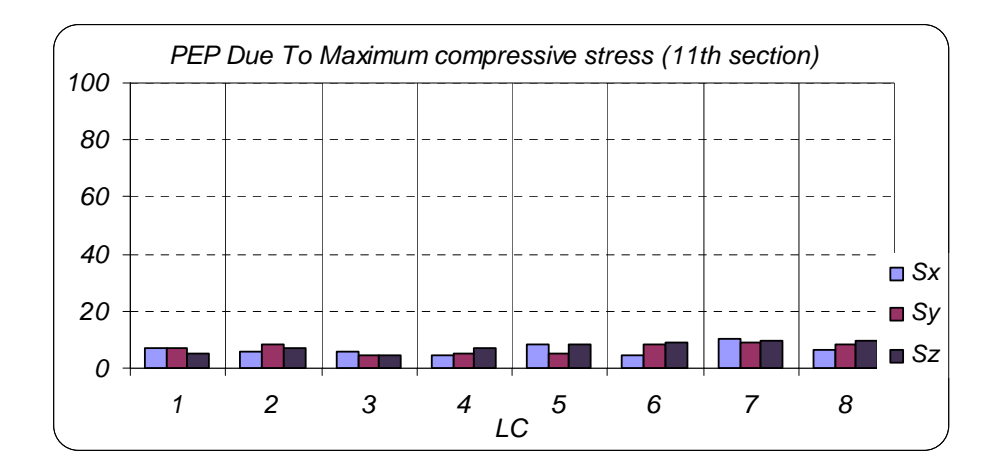


Fig. 15: PEP Due To Maximum compressive stress (11th section)

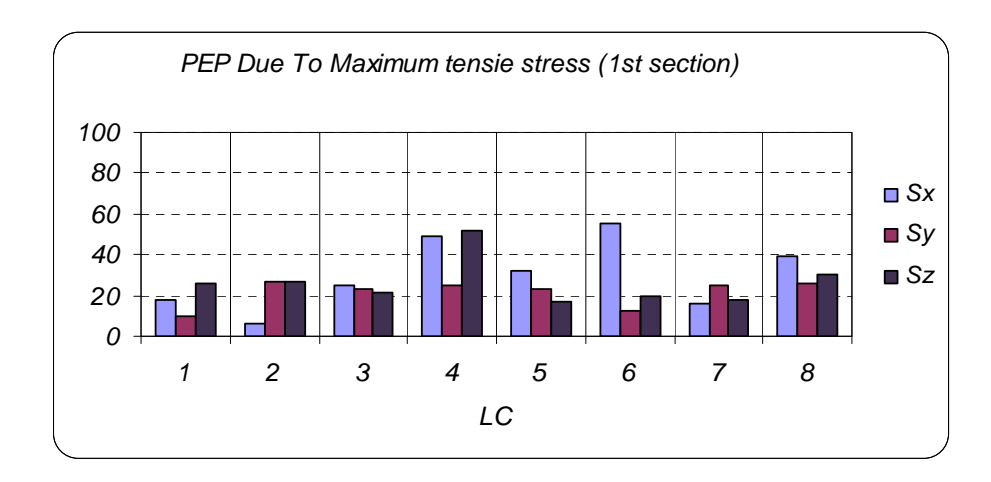


Fig. 16: PEP Due To Maximum Tensile stress (1st section)

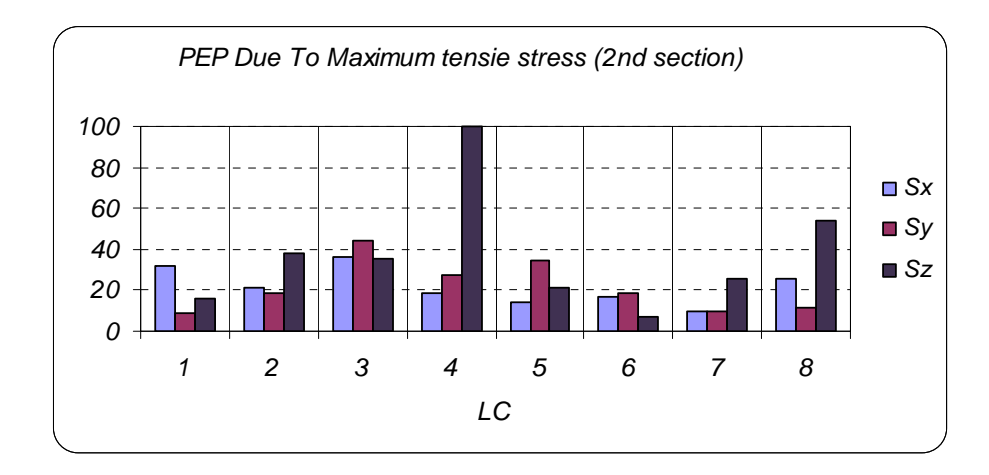


Fig. 17: PEP Due To Maximum Tensile stress (2nd section)

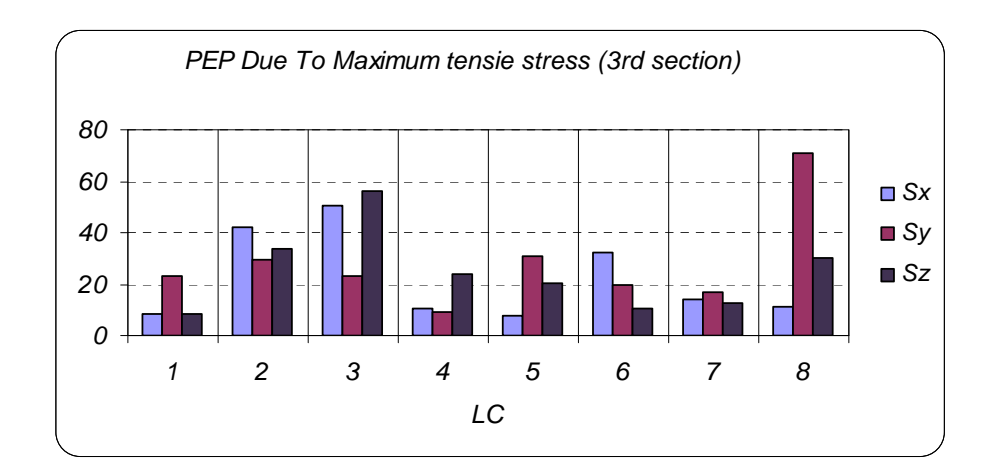


Fig. 18: PEP Due To Maximum Tensile stress (3rd section)

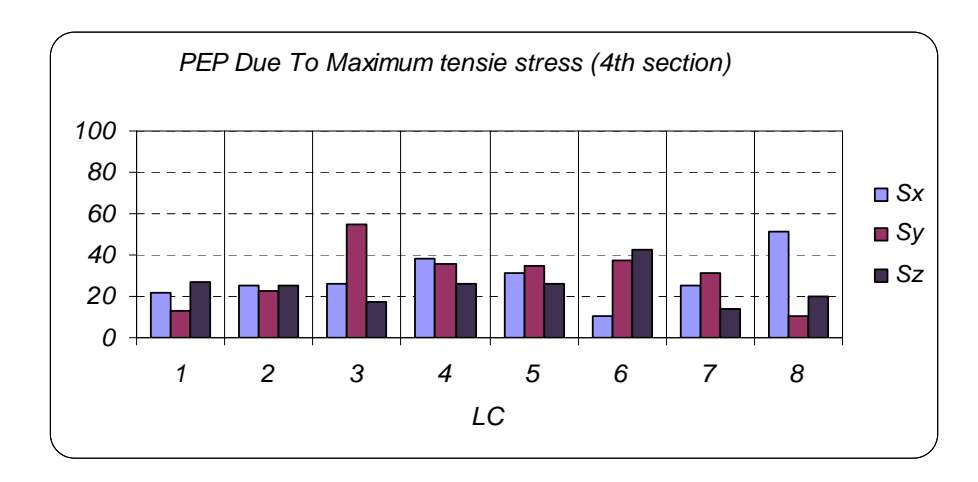


Fig. 19: PEP Due To Maximum Tensile stress (4th section)

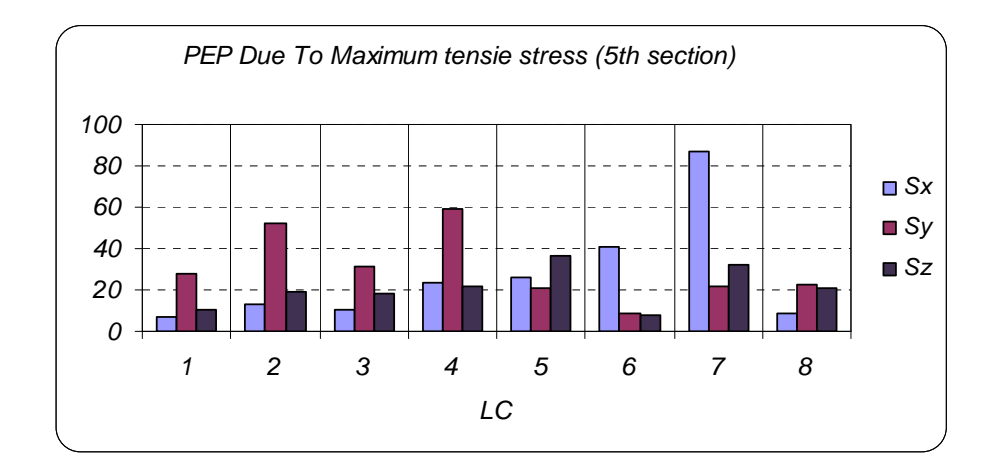


Fig. 20: PEP Due To Maximum Tensile stress (5th section)

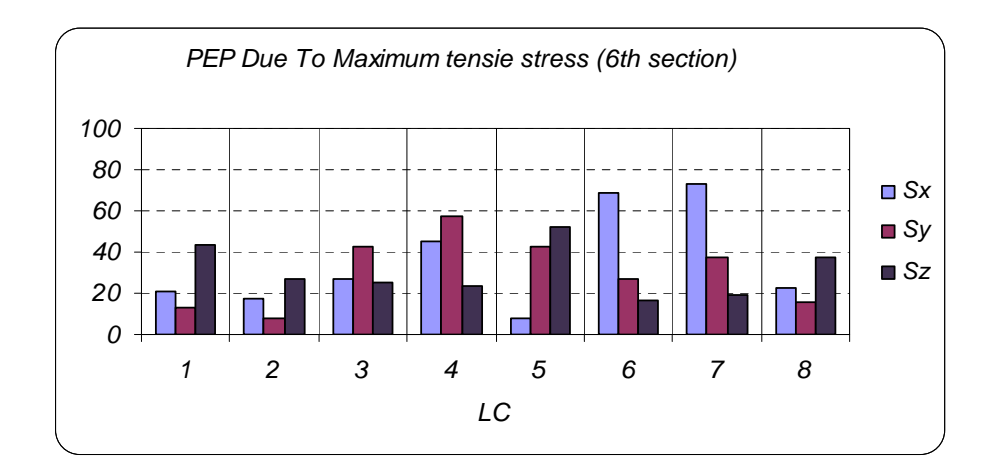


Fig. 21: PEP Due To Maximum Tensile stress (6th section)

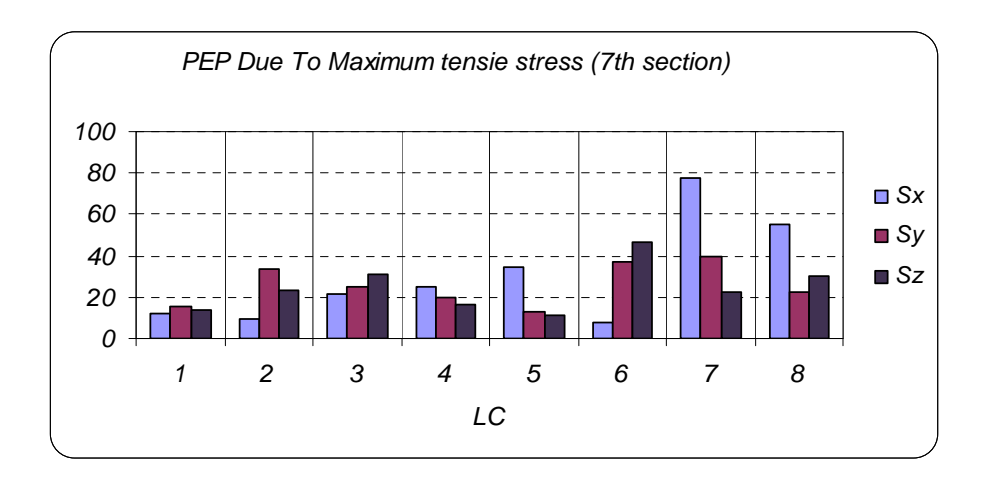


Fig. 22: PEP Due To Maximum Tensile stress (7th section)

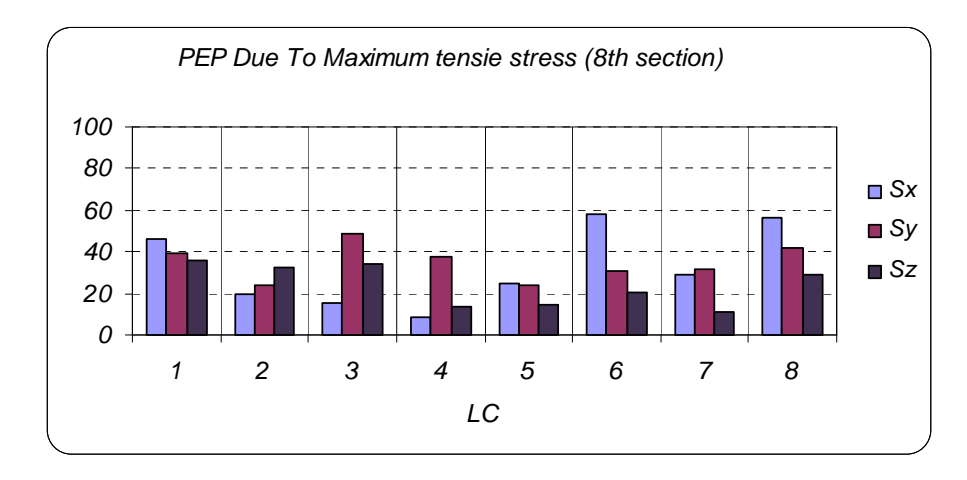


Fig. 23: PEP Due To Maximum Tensile stress (8th section)

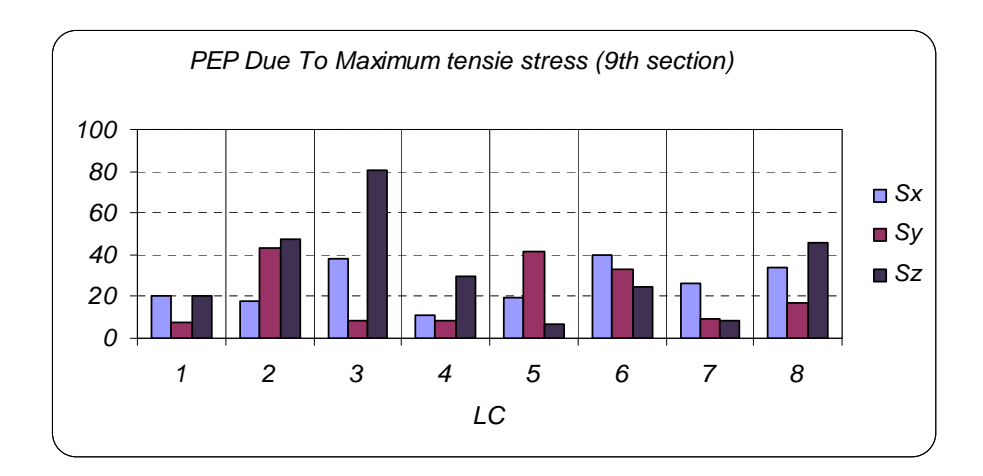


Fig. 24: PEP Due To Maximum Tensile stress (9th section)

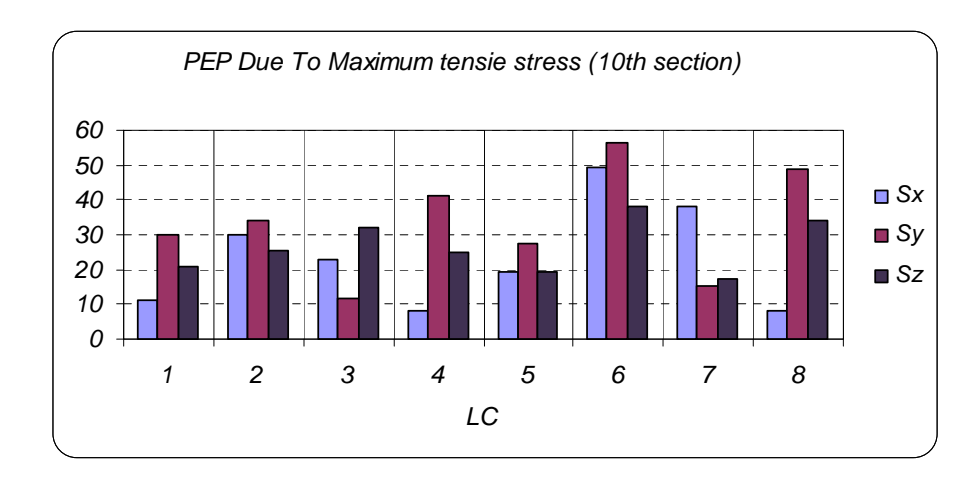


Fig. 25: PEP Due To Maximum Tensile stress (10th section)

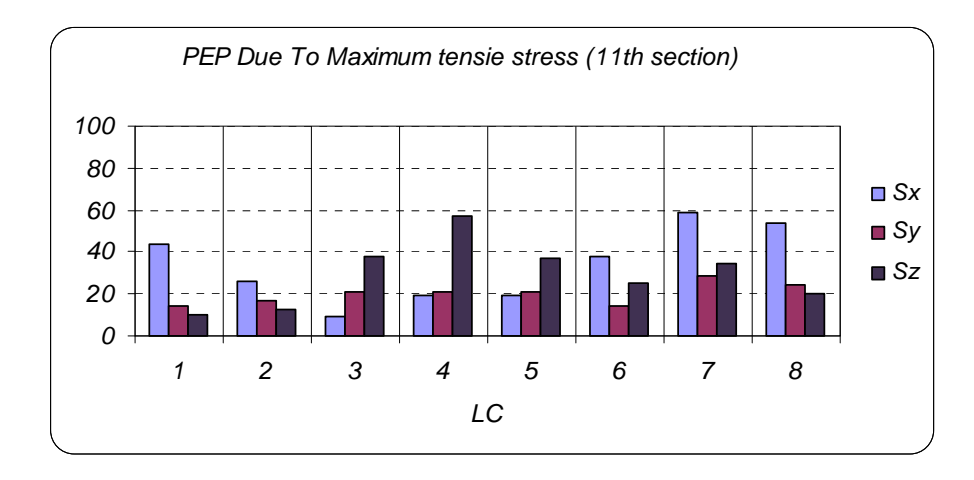


Fig. 26: PEP Due To Maximum Tensile stress (11th section)

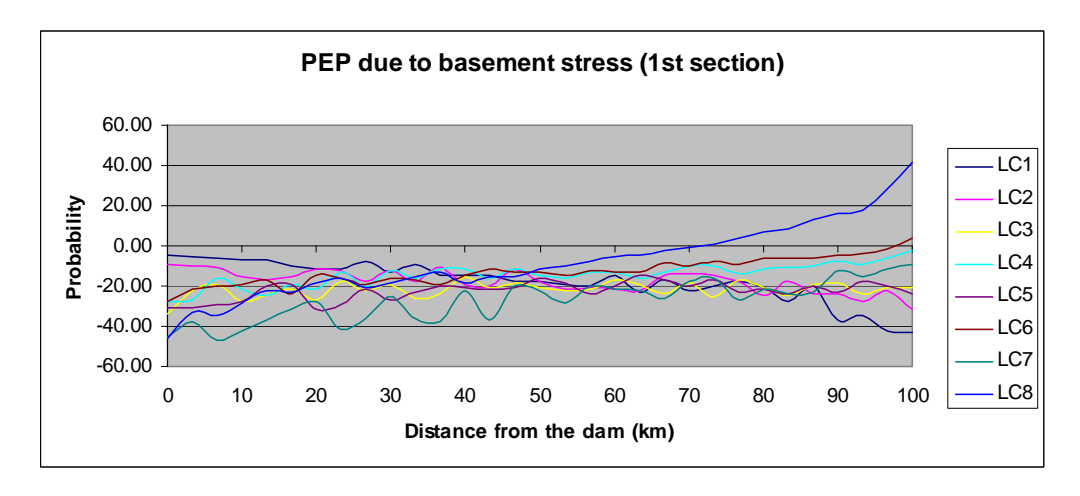


Fig. 27: PEP Due To Basement Stress (1st section)

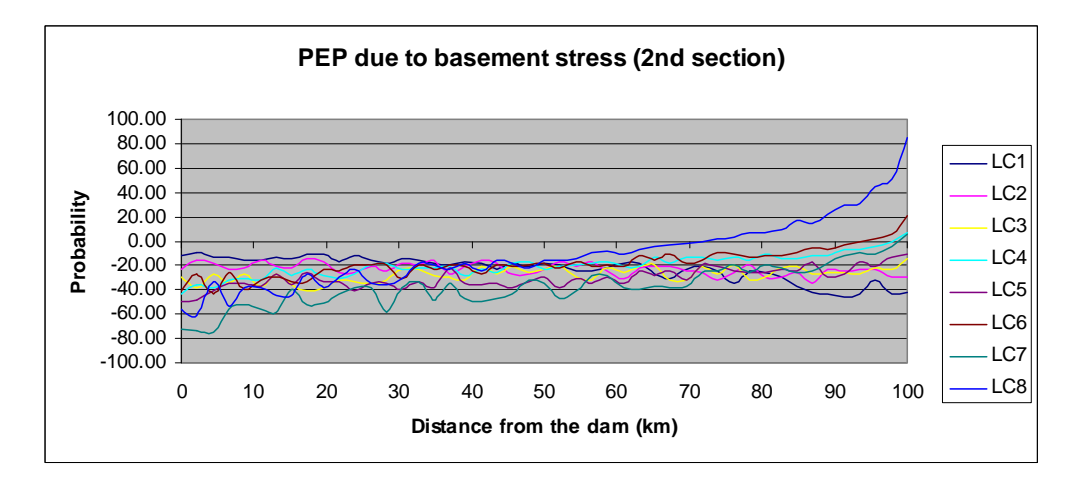


Fig. 28: PEP Due To Basement Stress (2nd section)

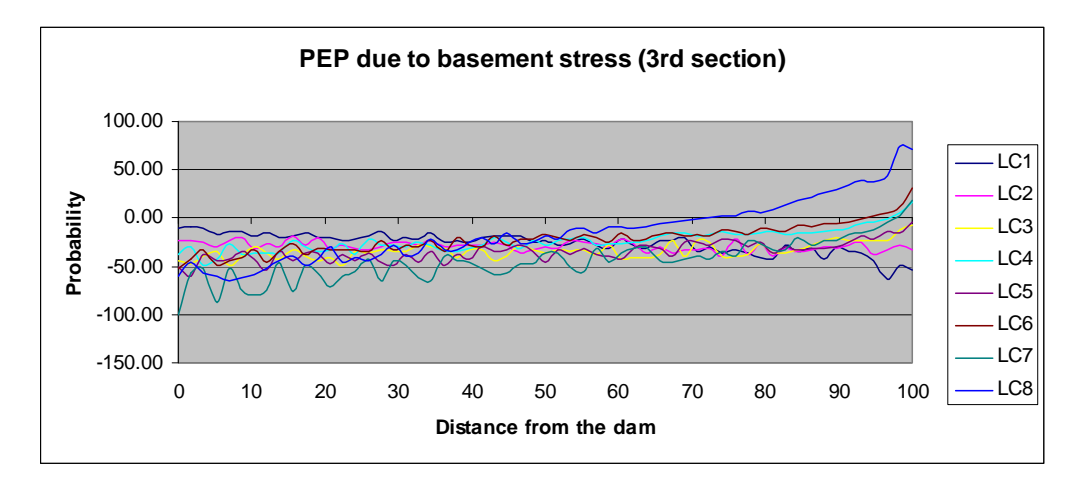


Fig. 29: PEP Due To Basement Stress (3rd section)

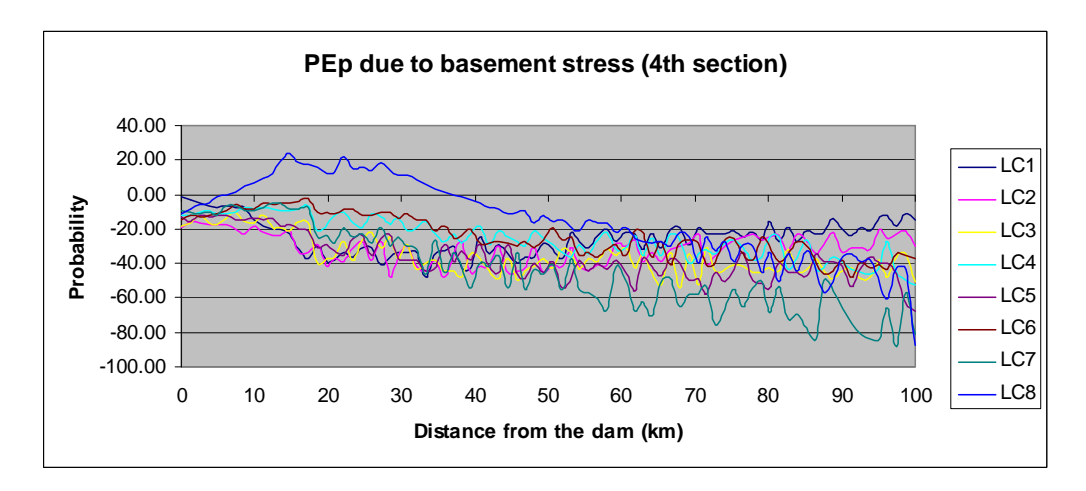


Fig. 30: PEP Due To Basement Stress (4th section)

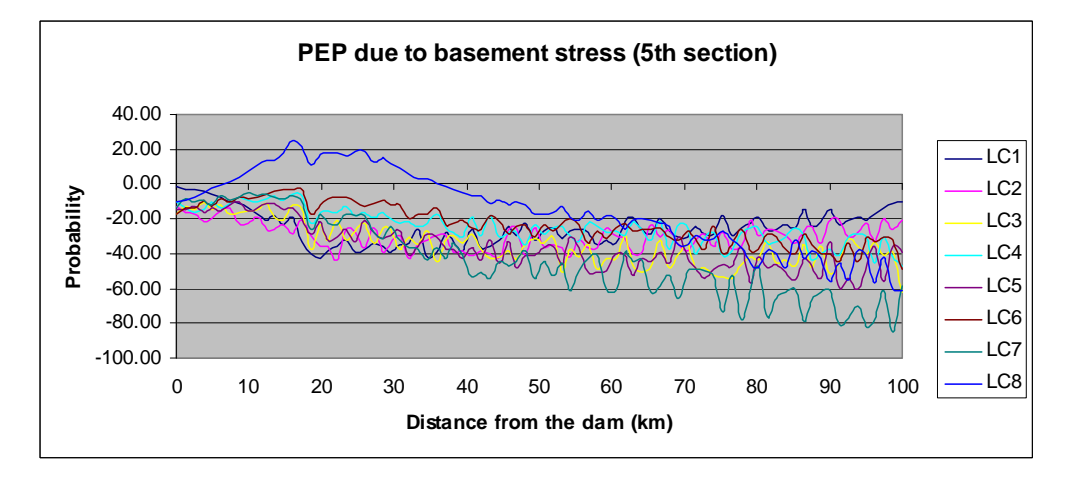


Fig. 31: PEP Due To Basement Stress (5th section)

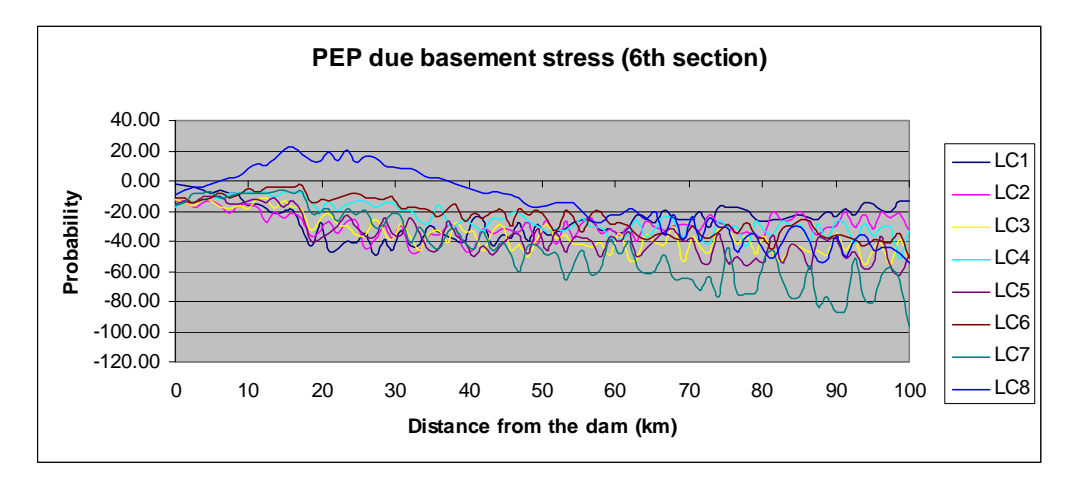


Fig. 32: PEP Due To Basement Stress (6th section)

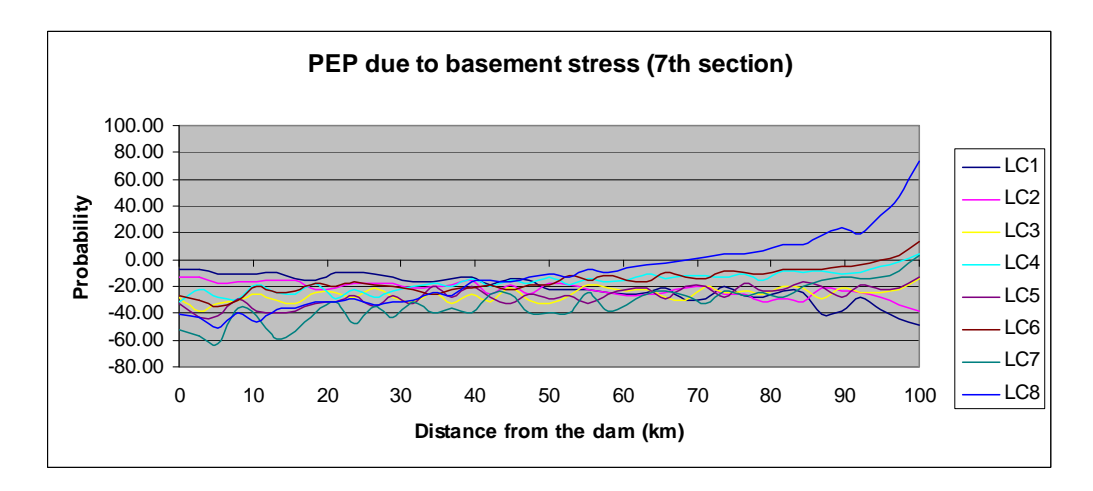


Fig. 33: PEP Due To Basement Stress (7th section)

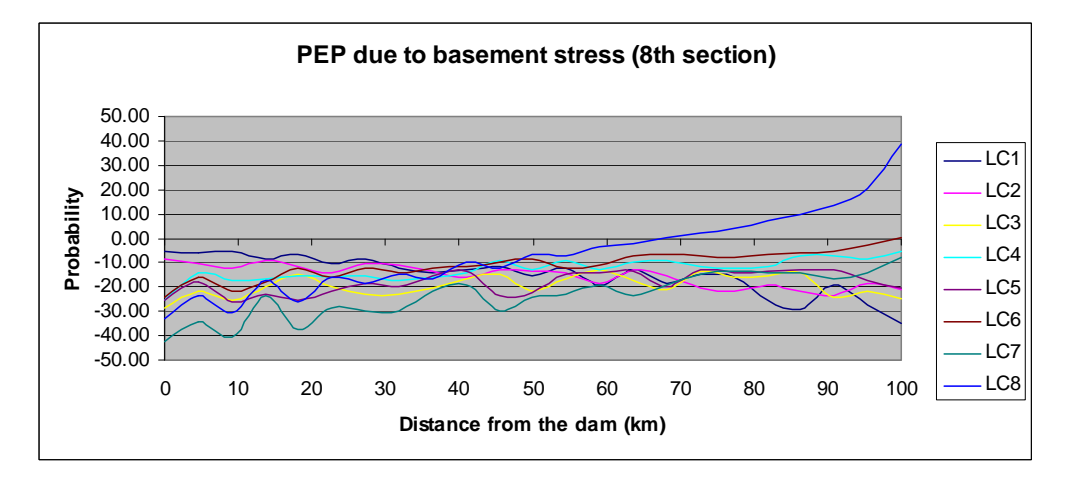


Fig. 34: PEP Due To Basement Stress (8th section)

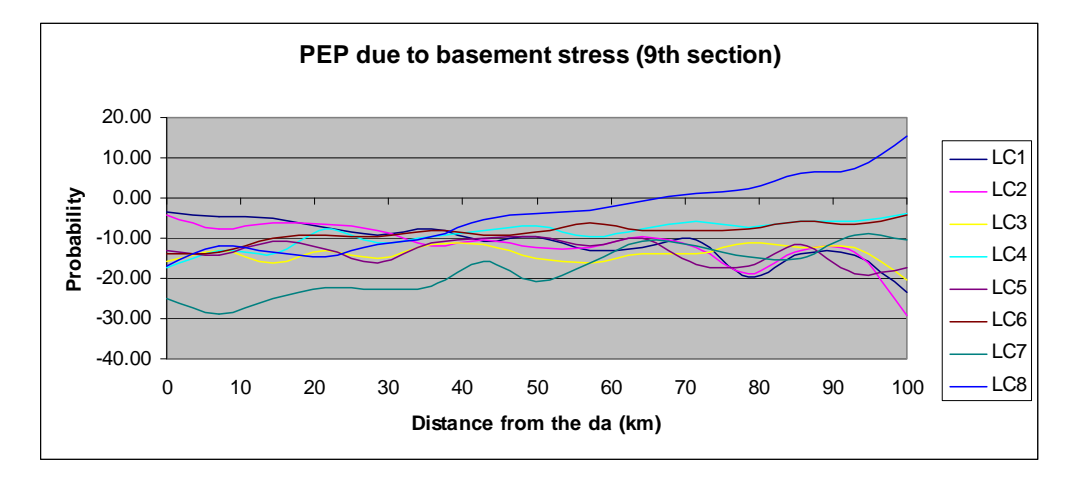


Fig. 35: PEP Due To Basement Stress (9th section)

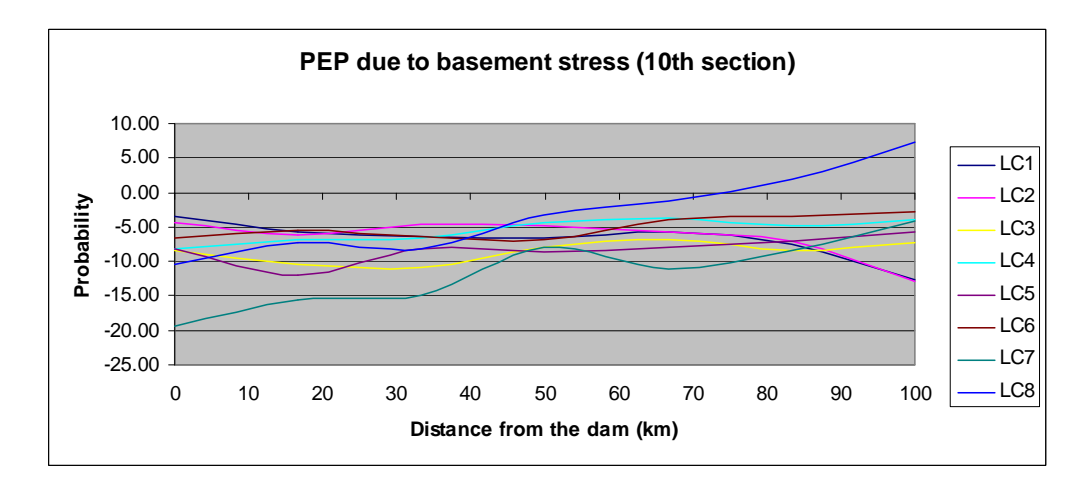


Fig. 36: PEP Due To Basement Stress (10th section)

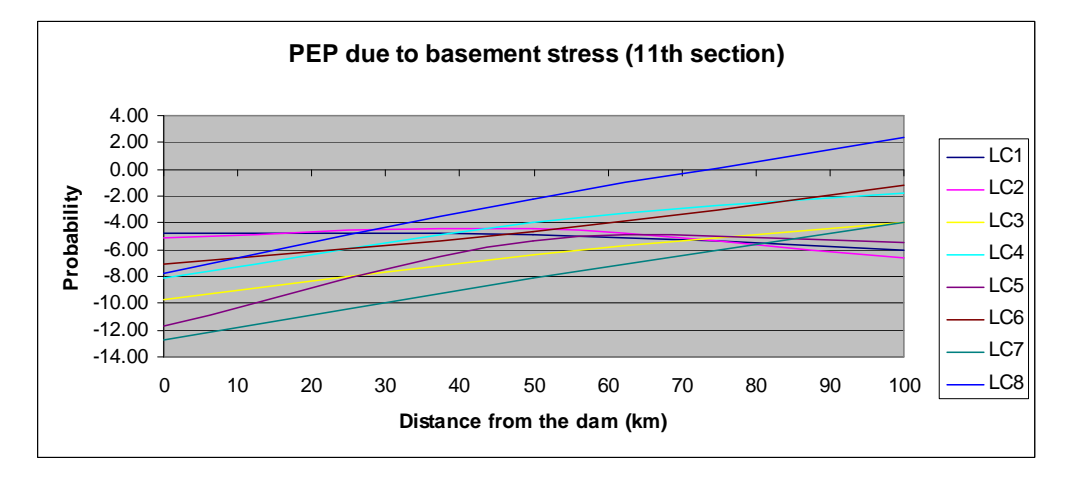


Fig. 37: PEP Due To Basement Stress (11th section)

Comparing Fig. 9 and Fig. 15, it is obvious that the PEP due to maximum compressive stress is not developed in the highest cross section of the dam. Also, comparing Fig. 20 and Fig. 22, it is clear that the PEP due to maximum tensile stress develops in D-D section which is smaller than E-E section. Thus, the highest cross section of the dam is not the most significant cross section for analyzing.

Moreover, Fig. 15 and Fig. 18 show that the PEP due to maximum compressive and the maximum tensile stress are not developed in the same cross section. That's why, as it is mentioned previously, all cross sections should be analyzed to determine the dam PEP due to seismic response.

According to the findings, S_y is always the determinant PEP due to compressive stress. In the other word, PEP due to stress along Y axis is the biggest compressive stress and it is bigger than both Sx and Sz. While, the determinant PEP due to tensile stress depends on the cross section geometry and loading condition (Fig. 16 and Fig. 20). However, in all sections S_x and S_y are normally bigger than S_z . And, S_z can never be a determinant. In normal loading condition, when there is no earthquake loading, the determinant PEP due to tensile stress is S_x , and S_y can be ignored.

The PEP due to stress distribution across the dam basement under different loading conditions for all cross sections are shown in Fig. 27 to Fig. 37. Even though the PEP due to stress distribution for different conditions extremely depend on the cross section geometry and loading condition but, they can be divided into the groups for similar cross section. For example, as it can be seen from Fig. 30 to Fig. 32, there are some similarities between PEP due to stress distribution changes for sections E-E to I-I.

In general, results show that when the earthquake accelerations are bigger, PEP due to maximum tensile stress at dam basement is increased. While, PEP due to the maximum compressive stress at dam basement depends on both earthquake acceleration and loading condition.

Fig. 29 shows that the PEP due to maximum tensile and compressive stress at dam basement develop at section D-D. Thus, the highest cross section is not the most important cross section and all sections of a inharmonic glen located RCC dam should be analyzed.

Conclusions:

In this paper, the probability of environmental pollution caused by Masjed soleyman dam failure is studied. Finite Element and ZENGAR methods are used to analyze the probability of pollution at dam downstream. Different dam cross sections and various loading conditions are considered to study the effects of these factors on the probability of environmental pollution due to seismic behavior of the dam. In general the results show that:

- (1) The PEP due to maximum compressive stress changes due to different loading conditions are similar for different cross sections. While, there is no response similarity for different cross sections and the PEP due to maximum tensile stress changes are vary from a cross section to another
- (2) The first modes of the earthquake, when earthquake inertia loading and the dam body weight act in the same direction, develop bigger PEP due to compressive stress. In addition, the second modes of the earthquake, when earthquake inertia loading and the dam body weight act in the opposite direction, develop bigger PEP due to tensile stress. Thus, for the environmental safety study of dams both modes of earthquake should be analyzed.
- (3) When the earthquake accelerations are bigger, both PEP due to maximum tensile and compressive stress of dam body are increased.
- (4) The PEP due to maximum compressive and tensile stresses are not developed in the highest cross section of the dam. Thus, the highest cross section of the dam is not the most significant cross section for analyzing.
- (5) PEP due to stress along Y axis (S_y) is always the determinant PEP due to compressive stress. While, in all sections S_x and S_y are the determinant PEP due to tensile stresses and normally they are bigger than S_z . And, S_z which can never be a determinant.
- (6) In normal loading condition, when there is no earthquake loading, the determinant PEP due to tensile stress is S_x , and S_y can be ignored.
- (7) Even though the PEP due to stress distribution for different conditions extremely depend on the cross section geometry and loading condition but, they can be divided into the groups for similar cross section.
- (8) Results show that when the earthquake accelerations are bigger, PEP due to maximum tensile stress at dam basement is increased. While, PEP due to the maximum compressive stress at dam basement depends on both earthquake acceleration and loading condition.

References

- Allahyari Pour, F., K. Mohsenifar and E. Pazira, 2011. Affect of Drought on Pollution of Lenj Station of Zayandehrood River by Artificial Neural Network (ANN). Advances in Environmental Biology, 5(7): 1461-1464.
- Arbabian, S. and M. Entezarei, 2011. Effects of Air Pollution on Allergic Properties of Wheat Pollens (Triticum aestivum). Advances in Environmental Biology, 5(7): 1480-1483.
- Arbabian, S., Y. Doustar, M. Entezarei and M. Nazeri, 2011. Effects of air pollution on allergic properties of Wheat pollens (Triticum aestivum). Advances in Environmental Biology, 5(6): 1339-1341.
- Chandrupatla, T. R., 1997. Introduction To Finite Elements In Engineering, Second Edition. Prentice Hall Inc.
- Fenves, G. and A.K. Chopra, 1984. Earthquake Analysis and Response of Concrete Gravity Dams: Report UCB/EERC-84/10. California University press.
- Hosseini, S.J. and M. Sadegh Sabouri, 2011. Adoption of Sustainable Soil Management by Farmers in Iran. Advances in Environmental Biology, 5(6): 1429-1432.
- Jianping, Zh., Y. Zeyan and Ch. Guanfu, 2006. Discussions on construction and type selection of China high dams. International Conference Hydropower, pp: 4-12.
- Mohsenifar, N., N. Mohsenifar and K. Mohsenifar, 2011. Using Artificial Neural Network (ANN) for Estimating Rainfall Relationship with River Pollution. Advances in Environmental Biology, 5(6): 1202-1208.
- Omran, M.E. and Z. Tokmechi, 2008. Parametric Study and Static and Pseudo static Analysis of Jehgin RCC Dam. University of Kurdistan Thesis.
- Qasim, M., H.M. Tayyab and E. Ahmad, 2010. Use of Salvage Wood for Reconstruction in Earthquake Affected Sites of Muzaffarabad, Azad Jammu & Kashmir. World Applied Sciences Journal, 8(7): 914-916.
- Qasim, M., M. Alam, B. Khan and E. Ahmad, 2010. Earthquake Induced Forest Damages in Balakot, Palas Valley, Muzaffarabad and Bagh Areas of North West Frontier Province and Azad Jammu and Kashmir Regions. World Applied Sciences Journal, 8(7): 912-913.
- United States Army Corps of Engineers, 1990. Earthquake Engineering for Concrete Dams: Design Performance and Research Needs. National Academy Press.
- United States Army Corps of Engineers, 1995. Gravity Dam Design, Report EM, 1110-2-2200. National Academy Press.
- Wang, H. and D. Li, 2006. Experimental study of seismic overloading of large arch dam. Earthquake Engineering & Structural Dynamics, 35(2): 199-216.